

AperTO - Archivio Istituzionale Open Access dell'Università di Torino

Phototransformation of the fungicide tebuconazole, and its relevance to sunlit surface freshwaters

This is the author's manuscript

Original Citation:

Availability:

This version is available <http://hdl.handle.net/2318/1878501> since 2022-11-03T17:35:35Z

Published version:

DOI:10.1016/j.chemosphere.2022.134895

Terms of use:

Open Access

Anyone can freely access the full text of works made available as "Open Access". Works made available under a Creative Commons license can be used according to the terms and conditions of said license. Use of all other works requires consent of the right holder (author or publisher) if not exempted from copyright protection by the applicable law.

(Article begins on next page)

1 **Phototransformation of the fungicide tebuconazole, and its predicted fate in**
2 **sunlit surface freshwaters**

3
4 **Luca Carena, Andrea Scozzaro, Monica Romagnoli, Marco Pazzi, Luca Martone,**
5 **Claudio Minero, Marco Minella, Davide Vione***

6
7 *Dipartimento di Chimica, Università degli Studi di Torino, Via Pietro Giuria 5, 10125 Torino,*
8 *Italy.*

9 * Corresponding author. *davide.vione@unito.it*

10

11 ***Abstract***

12 The fungicide tebuconazole (TBCZ) is expected to undergo negligible direct photolysis in surface
13 freshwaters, but it can be degraded by indirect photochemistry. TBCZ mainly reacts with hydroxyl
14 radicals and, to a lesser extent, with the triplet states of chromophoric dissolved organic matter
15 (³CDOM*). Indirect photochemistry is strongly affected by environmental conditions, and TBCZ
16 lifetimes of about one week are expected in sunlit surface waters under favourable circumstances
17 (shallow waters with low concentrations of dissolved organic carbon, DOC, during summer). In
18 these cases the time trend would follow pseudo-first order kinetics (mono-exponential decay).
19 Under less favourable conditions, photoinduced degradation would span over a few or several
20 months, and TBCZ phototransformation would depart from an exponential trend because of
21 changing sunlight irradiance. The TBCZ phototransformation products should be less toxic than
22 their parent compound, thereby providing potential for photodegradation to decrease the
23 environmental impact of TBCZ. Hydroxylation is a major TBCZ transformation route, due to either
24 •OH attack, or one-electron oxidation sensitised by ³CDOM*, followed by reaction of the oxidised
25 transient with oxygen and water.

26

27 **Keywords:** tebuconazole; surface-water photochemistry; direct photolysis; dissolved organic
28 matter; transformation pathways.

29

30 **Introduction**

31

32 Tebuconazole((RS)-1-p-chloro-phenyl-4,4-dimethyl-3-(1H-1,2,4-triazol-1-ylmethyl)pentan-3-ol),
33 hereinafter TBCZ, is a broad-spectrum triazole fungicide that is widely used for the protection of
34 orchards, vegetables, cereals, and lawns (Miyauchi et al., 2005; Clausen and Yang, 2007; Lyu et al.,
35 2018). It is used as both seed dressing and foliar spray, and it acts on fungi by blocking the
36 biosynthesis of sterols. TBCZ inhibits the demethylation process that takes place on the cellular
37 membrane of these pathogenic organisms (Paul et al., 2008; Fera et al., 2009).

38 TBCZ has moderate to low toxicity towards mammals, but it is peculiarly toxic to aquatic life forms
39 (EFSA, 2008). Moreover, it is classified as type C human carcinogen (possibly carcinogenic to
40 humans) (Želonková et al., 2019), and has potential to cause endocrine-disrupting effects (Yu et al.,
41 2013). The persistence of TBCZ in soil is highly variable (Muñoz-Leoz et al., 2011), and TBCZ
42 might also be resistant to biodegradation in the aquatic environment (Boethling et al., 2004). TBCZ
43 has been detected in surface waters at ng L⁻¹ levels, and even in wastewater at some tens ng L⁻¹,
44 although there are arguably additional routes than wastewater for TBCZ to enter the water
45 environment (most notably, runoff from soil as well as urban areas) (Kahle et al., 2008).

46 Past studies have excluded direct photolysis, as a significant transformation route of TBCZ in
47 surface waters, due to insignificant absorption of sunlight (Coody, 1987). The direct photolysis is
48 the transformation of a compound triggered by photon absorption (Yan and Song, 2014) but,
49 although it can be an important process for some substances, it is not the only phototransformation
50 pathway for a contaminant in surface waters. Indirect photochemistry is another potentially
51 important route, in which sunlight is absorbed by naturally occurring compounds called

52 photosensitisers (Remucal, 2014). The main photosensitisers in surface waters are nitrate, nitrite,
 53 and the chromophoric dissolved organic matter (CDOM) (Dong and Rosario-Ortiz, 2012; Mostafa
 54 and Rosario-Ortiz, 2013; Vione and Scozzaro, 2019). Radiation absorption by photosensitisers
 55 triggers the generation of photochemically produced reactive intermediates (PPRIs), such as the
 56 hydroxyl radicals ($\bullet\text{OH}$), singlet oxygen ($^1\text{O}_2$), and CDOM triplet states ($^3\text{CDOM}^*$). PPRIs can
 57 react with contaminants. and cause their degradation (Vione et al., 2014). Moreover, the oxidation
 58 of $\text{HCO}_3^-/\text{CO}_3^{2-}$ by $\bullet\text{OH}$, and of CO_3^{2-} by $^3\text{CDOM}^*$ produces the carbonate radical, $\text{CO}_3^{\bullet-}$, as a
 59 further PPRI (Canonica et al., 2005; Yan et al., 2019). The different PPRIs reach relatively low
 60 steady-state concentrations in surface waters ($10^{-18} - 10^{-13}$ M) (Rosario-Ortiz and Canonica, 2016),
 61 due to the budget between photogeneration and scavenging/quenching (Vione et al., 2014). Indeed,
 62 $\bullet\text{OH}$ is generated by irradiation of nitrate, nitrite, and CDOM, and it is scavenged by DOM
 63 (dissolved organic matter, not necessarily chromophoric), inorganic carbon ($\text{HCO}_3^-/\text{CO}_3^{2-}$), as well
 64 as bromide in saltwater and seawater (Gligorovski et al., 2015). DOM is also the main scavenger for
 65 $\text{CO}_3^{\bullet-}$ (Yan et al., 2019), but it is unable to quench significant fractions of $^3\text{CDOM}^*$ or $^1\text{O}_2$, unless
 66 the values of the water dissolved organic carbon (DOC) are very high (Cory et al., 2009; Wenk et
 67 al., 2013). Therefore, the main $^3\text{CDOM}^*$ sink is dissolved O_2 , and the reaction between $^3\text{CDOM}^*$
 68 and O_2 is the only significant $^1\text{O}_2$ source (~50% yield) (McNeill and Canonica, 2016). Finally, $^1\text{O}_2$
 69 is mainly quenched by collision with water (Wilkinson and Brummer, 1981).
 70 Although DOM is usually unable to significantly scavenge $^3\text{CDOM}^*$, its antioxidant (mostly
 71 phenolic) moieties can inhibit the photodegradation of some contaminants, which have initially
 72 been oxidized by $^3\text{CDOM}^*$ and/or $\text{CO}_3^{\bullet-}$ (Canonica and Laubscher, 2008; Carena et al., 2022).
 73 Indeed, $^3\text{CDOM}^*$ and $\text{CO}_3^{\bullet-}$ degrade contaminants by electron or H-atom abstraction and,
 74 depending on reduction potential and reaction kinetics, the transient species resulting from initial
 75 pollutant oxidation may be back-reduced to the starting compound by the phenolic moieties

76 contained in DOM (Wenk et al., 2011; Wenk and Canonica, 2012; Hao et al, 2020; Carena et al.,
77 2022).

78 The reaction between PPRIs and contaminants is usually a minor pathway for PPRI dissipation, but
79 it can have a key role in contaminant fate (Remucal, 2014; Vione et al., 2014; Baena-Nogueras et
80 al., 2017). Indeed, indirect photochemistry adds to the direct photolysis in photodegradation of
81 sunlight-absorbing contaminants, and it is the only possible phototransformation route for
82 compounds that do not absorb sunlight. It is actually very rare for contaminants not to undergo
83 indirect photodegradation (most compounds should react at least with the very strong oxidant $\bullet\text{OH}$;
84 Buxton et al., 1988). However, the kinetics and environmental importance of the indirect
85 photochemistry process(es) have to be assessed on a case-by-case basis.

86 To this purpose, the main goal of this work is the assessment of the overall photodegradation
87 kinetics and pathways of TBCZ, with a particular emphasis on indirect photochemistry. The
88 assessment is carried out by a combination of photodegradation experiments and photochemical
89 modelling. The latter is important, on the one side, to understand which photodegradation lifetimes
90 can be expected for TBCZ in different environmental conditions; on the other hand, modelling
91 gives insight into the peculiar photochemical pathways that are more important for TBCZ in the
92 environment, and that may produce key transformation products. By so doing, product
93 identification can be focused on the main expected phototransformation routes (Gornik et al., 2021).

94

95 **Materials and methods**

96

97 *Chemicals and solvents*

98 Chemicals used in this study were of analytical grade. Solvents and eluents were of gradient-grade
99 purity for liquid chromatography. A detailed list that specifies purity grade and supplier for each
100 reagent is provided in **Text S1 (SM)**. Ultra-pure water was of Milli-Q quality (18.5 MΩ cm, TOC <
101 2 ppb).

102

103 *Irradiation experiments*

104 Different irradiation set-ups and different solutions were used for the study of TBCZ
105 photoreactivity. Direct photolysis was studied by irradiating TBCZ alone under a UVB lamp
106 (Philips narrow band TL 20W/01, emission maximum at 313 nm). The same lamp was used to
107 study the reaction kinetics between TBCZ and $\bullet\text{OH}$, by irradiating TBCZ together with H_2O_2 as
108 $\bullet\text{OH}$ source. The $\bullet\text{OH}$ scavenger 2-propanol was added at different concentration values, to achieve
109 competition kinetics with TBCZ, and determine the second-order reaction rate constant between
110 TBCZ and $\bullet\text{OH}$.

111 The reaction between TBCZ and $\text{CO}_3^{\bullet-}$ was studied by UVB irradiation of mixtures of TBCZ +
112 $\text{NaNO}_3 + \text{NaHCO}_3$, TBCZ + NaNO_3 + phosphate buffer (at the same total concentration and pH as
113 the NaHCO_3 -containing solutions), and TBCZ + NaHCO_3 (blank experiment, to check for the direct
114 photolysis of TBCZ). The initial concentration values were: 20 μM TBCZ; 10 mM NaNO_3 (when
115 present), as well as 0, 5, or 11 mM NaHCO_3 (or phosphate buffer). The rationale here is that
116 irradiated NaNO_3 yields $\bullet\text{OH}$, which in the presence of NaHCO_3 oxidises $\text{HCO}_3^-/\text{CO}_3^{2-}$ to $\text{CO}_3^{\bullet-}$.
117 The comparison of TBCZ degradation rates, in the three different systems, indicates whether or not
118 the reaction with $\text{CO}_3^{\bullet-}$ is significant (Vione et al., 2009). The choice of nitrate instead of H_2O_2 in
119 this series of experiments is motivated by the need of exploiting a solvent-cage effect, which

120 involves the geminate species produced by nitrate photolysis (Vione et al., 2011, and see the
121 Supplementary Material for further details).

122 The triplet photosensitiser 4-carboxybenzophenone (CBBP, in its deprotonated anionic form) was
123 used as CDOM proxy, due to similar reactivity between the triplet states $^3\text{CBBP}^*$ and $^3\text{CDOM}^*$
124 (Avetta et al., 2016). Irradiation of mixtures of TBCZ and CBBP was carried out under a UVA
125 black lamp (Philips TL-D 18 W, with emission maximum at 369 nm), under which conditions
126 CBBP can be selectively excited.

127 The reaction between TBCZ and $^1\text{O}_2$ was studied by using the dye Rose Bengal as $^1\text{O}_2$ source, upon
128 irradiation under a yellow lamp (TL D 18W/16 Yellow). Excited Rose Bengal in its triplet state
129 transfers energy to ground-state O_2 , to produce $^1\text{O}_2$ (DeRosa and Crutchley, 2002).

130 Chemical actinometry with 2-nitrobenzaldehyde (Carena et al., 2019; Galbavy et al., 2010; Willett
131 and Hites, 2000) was used, together with the lamp emission spectra (taken with an Ocean Optics
132 USB 2000 CCD Spectrophotometer) to determine the spectral photon flux density occurring in the
133 irradiated solutions. The emission spectra thus obtained for the three lamps are reported in **Figure**
134 **S1 (SM)**.

135 During irradiation, the aqueous solutions (5 or 20 mL, pH ranging from 6 to 7 except for the
136 $\text{NaNO}_3/\text{HCO}_3^-$ ($\text{CO}_3^{\bullet-}$) experiments, where it reached up to 8.5) were introduced into cylindrical
137 Pyrex glass cells, tightly closed with a screw cap, and magnetically stirred. Pyrex glass has a cut-off
138 wavelength around 290 nm, thus it transmits >50% radiation above 300 nm (see **Figure S2 (SM)**).
139 Anyway, radiation absorption by Pyrex was taken into account in actinometry experiments.

140

141 ***Monitoring of TBCZ photodegradation***

142 After the scheduled irradiation time, each cell was withdrawn from the lamp, and its contents were
143 analysed by high-performance liquid chromatography coupled with diode array detection (HPLC-
144 DAD), to quantify residual TBCZ. The used instrument was a VWR-Hitachi Chromaster, equipped
145 with 5260 autosampler (60 μL injection volume), 5160 quaternary pump, and 5430 DAD detector.

146 The column was a Merck LiChroCART RP-18 cartridge (125 mm × 4 mm × 5 μm). Isocratic
147 elution was carried out with a 75:25 mixture of methanol and acidified water (H₃PO₄, pH 2.8). The
148 eluent flow rate was 1 mL min⁻¹, which under the reported conditions produced a TBCZ retention
149 time of 5.4 min. The detection wavelength was 221 nm.

150 The TBCZ time trends followed pseudo-first order kinetics, and could be fitted with the equation
151 $C_{\text{TBCZ}} = C^{\circ}_{\text{TBCZ}} e^{-k t}$, where C_{TBCZ} is the concentration of TBCZ at the time t , C°_{TBCZ} the initial
152 TBCZ concentration, and k its pseudo-first order photodegradation rate constant. The initial rate of
153 TBCZ photodegradation was $R_{\text{TBCZ}} = k C^{\circ}_{\text{TBCZ}}$.

154

155 *Identification of TBCZ phototransformation products*

156 The TBCZ phototransformation products were identified by high-performance liquid
157 chromatography, coupled with diode array detection and mass spectrometry (HPLC-DAD-MS). A
158 Thermo Scientific Accela chromatograph was used, equipped with Accela autosampler (20 μL
159 injection volume), a quaternary Accela pump, and DAD Accela PDA detector. The column used
160 was a Phenomenex Synergi Polar-RP 80A cartridge (150 mm × 2 mm × 4 μm), which was
161 maintained at 30 °C. The mass spectrometer was a Thermo LCQ Fleet (ion-trap) Mass
162 Spectrometer, equipped with electrospray ionisation (ESI). Elution was carried out in binary
163 gradient mode. The mobile phase consisted of formic acid 0.1% (v/v; eluent A), and methanol
164 (eluent B). The following gradient program (time, %A/%B) was applied: 0 min, 95/5; 20 min,
165 0/100; 30 min, 0/100; 30.1 min, 95/5; 35 min, 95/5. The flow rate was 0.2 mL min⁻¹. The DAD
166 detection wavelength was 221 nm.

167 The initial Full Scan analysis was carried out in positive ion mode. It gave the characteristic ions,
168 on which the successive MSⁿ analyses were carried out. The collision energy was chosen each time
169 between 25 or 35 eV, and the different values used for the identification of each relevant ion are
170 reported in **Table S1 (SM)**.

171

172 *Modelling of TBCZ phototransformation in surface freshwaters*

173 TBCZ photodegradation kinetics and pathways in surface freshwaters were modelled with the
174 APEX software (Bodrato and Vione, 2014), which has proven its suitability to assess the
175 photochemical fate of contaminants in environmental aqueous systems (Avetta et al., 2016). APEX
176 requires as input data both the chemical and photochemical features of a water body (i.e.,
177 concentration of photosensitisers and reactive species scavengers, water absorption spectrum and
178 water depth, of which reasonable values were assumed), and the photoreactivity parameters of the
179 considered contaminant (UV-visible absorption spectrum, direct photolysis quantum yield, and
180 second-order reaction rate constants with $\bullet\text{OH}$, $\text{CO}_3^{\bullet-}$, $^1\text{O}_2$, and $^3\text{CDOM}^*$). The output values of
181 photodegradation kinetics (pseudo-first order photodegradation rate constants, k , and half-life times,
182 $t_{1/2}$) are average values over a water column of given depth (Bodrato and Vione, 2014). The main
183 goal of the irradiation experiments, carried out in this work, was to provide the contaminant input
184 data for APEX (TBCZ quantum yield for direct photolysis, as well as second-order reaction rate
185 constants with PPRIs; see **Table S2 (SM)**), not to directly simulate environmental photochemistry
186 conditions.

187 The APEX software was initially run supposing a clear-sky scenario, corresponding to July, 15th, at
188 45°N latitude. In this way, the time unit obtained as output corresponds to a 24-h day, which takes
189 the day-night cycle into account. Seasonal variability of photodegradation was obtained by means
190 of the *APEX_Season* function (Bodrato and Vione, 2014), which returns first-order
191 photodegradation rate constants in different months of the year. The latter approach has interesting
192 implications for the time trend of a contaminant. Actually, quite complete (~95%) contaminant
193 photodegradation can be achieved in one month, if the first-order lifetime is around a week ($t_{1/2} \sim 7$
194 days, which corresponds to $k \sim 0.1 \text{ day}^{-1}$). In case of longer lifetimes, photodegradation continues in
195 the following month(s), when the pollutant experiences different conditions of sunlight irradiance.
196 This issue decreases the accuracy of a description, based on a single (and monthly-based) first-order
197 photodegradation rate constant. It has been shown recently (Vione, 2021) that the resulting time

198 trend can be well approximated by a series of first-order tracts, each lasting for one month: in fact,
 199 in a month's time the irradiance conditions do not vary much, under the hypothesis of consistent
 200 fine weather. The approximated trend is described by the following equation (Vione, 2021):

$$201 \quad C_t / C_o = \prod_{m=0}^M e^{-k_m \Delta t_m} \quad (1)$$

202 where $m = 0$ is the initial month of pollutant emission, m a generic month, M the total number of
 203 months included in the simulation, k_m (day^{-1} units, as returned by *APEX-season*) the pseudo-first
 204 order degradation rate constant of the contaminant in the month m , and $\Delta t_m = 28, 30$, or 31 days,
 205 depending on the month. Moreover, C_o is the initial contaminant concentration ($m = 0$), and C_t is the
 206 concentration at the end of the month M . In these simulations, it was assumed that water chemistry
 207 and depth did not vary over time. The rationale for this assumption is that seasonal variations of the
 208 irradiance play a much more important role in the photodegradation of contaminants, than the
 209 typical, corresponding variations in water chemistry and depth (Vione, 2021).

210 The ECOSAR software (Mayo-Bean et al., 2012) was finally used, to assess the acute and chronic
 211 toxicity of TBCZ, and of its detected phototransformation products. By means of a quantitative
 212 structure-activity relationship approach, ECOSAR can predict the acute and chronic toxicity (LC50,
 213 EC50, chronic values ChV) for freshwater organisms such as fish, daphnid (crustaceans), and algae.
 214 Concerning accuracy, a compound can be said to be more toxic than another when the predicted
 215 values differ by at least an order of magnitude (Mayo-Bean et al., 2012).

216

Results and Discussion

Direct photolysis of TBCZ

Solutions (20 mL) containing 5 μM TBCZ were irradiated for up to 70 h under the UVB lamp. The choice of this lamp was motivated by the fact that TBCZ absorbs sunlight mostly in the UVB region, and with very low absorption coefficients (around or below $1 \text{ M}^{-1} \text{ cm}^{-1}$ at $\lambda > 300 \text{ nm}$, see **Figure 1**). While previous reports have indicated that TBCZ does not absorb sunlight (Coody, 1987), our results suggest that sunlight absorption by TBCZ would be, if not totally negligible, at least extremely low.

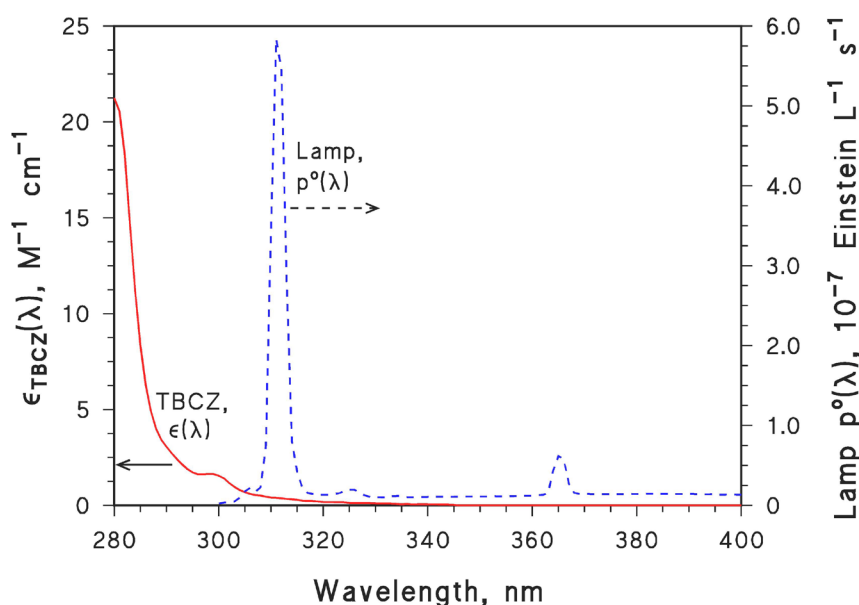


Figure 1. *Left Y-axis:* absorption spectrum of TBCZ (molar absorption coefficient, $\varepsilon_{\text{TBCZ}}(\lambda)$). *Right y-axis:* emission spectrum of the Philips TL 20W/01 UVB lamp (spectral photon flux density, $p^\circ(\lambda)$).

The initial degradation rate of TBCZ in these conditions was $R_{\text{TBCZ}} = (3.46 \pm 0.40) \times 10^{-12} \text{ M s}^{-1}$ (mean \pm standard error of experiments run in duplicate). The fraction of TBCZ degraded after 70 h continuous irradiation was as low as 17%, which indeed suggests a limited importance of the direct photolysis process. At the same time, negligible degradation was detected in dark experiments

235 where 5 μM TBCZ was placed under the same lamp, using the same irradiation cells wrapped in
 236 aluminium foil, to attain comparable temperature and stirring conditions as for the irradiation
 237 experiments.

238 By excluding dark processes such as hydrolysis, in agreement with previous reports (Wiche and
 239 Bogdoll, 2007), the degradation of TBCZ observed under irradiation could be attributed to direct
 240 photolysis alone. The direct photolysis quantum yield of TBCZ can be calculated as the ratio
 241 between R_{TBCZ} and the photon flux absorbed by TBCZ, as follows (Braslavsky, 2007):

$$242 \quad \Phi_{\text{TBCZ}} = \frac{R_{\text{TBCZ}}}{\int_{\lambda} p^{\circ}(\lambda) [1 - 10^{-\varepsilon_{\text{TBCZ}}(\lambda) b C^{\circ}_{\text{TBCZ}}]} d\lambda} = 0.22 \pm 0.03 \quad (2)$$

243 where R_{TBCZ} is the initial degradation rate of TBCZ by direct photolysis, $\varepsilon_{\text{TBCZ}}$ its molar absorption
 244 coefficient, $b = 1.6$ cm the optical path length of radiation in the solution inside the irradiation cells,
 245 and $C^{\circ}_{\text{TBCZ}} = 5$ μM (TBCZ initial concentration). The values of $p^{\circ}(\lambda)$ (lamp spectral photon flux
 246 density) are those reported in **Figure 1**, which also shows the values of $\varepsilon_{\text{TBCZ}}(\lambda)$. Integration was
 247 carried out between 300 and 330 nm, where the spectra of TBCZ and the lamp overlap.

248

249 **Reaction between TBCZ and $\bullet\text{OH}$**

250 The reaction rate constant between TBCZ and $\bullet\text{OH}$ was determined by means of competition
 251 kinetics with 2-propanol (2-Prop), using H_2O_2 under UVB irradiation as the photochemical source
 252 of $\bullet\text{OH}$ (Zellner et al., 1990). These irradiation conditions are known to trigger some direct
 253 photolysis of TBCZ (*vide supra*), thus the reaction system can be outlined as follows (Buxton et al.,
 254 1988; Gligorovski et al., 2015):



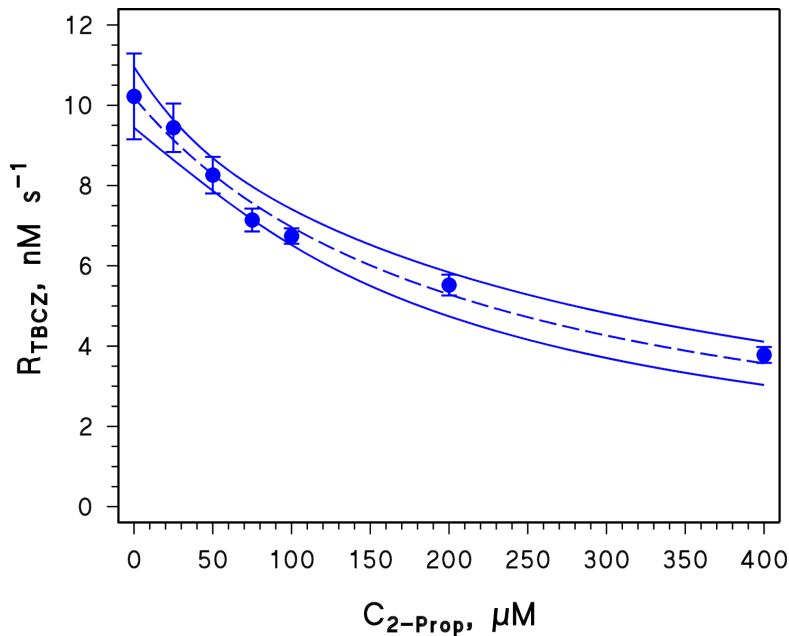


260 Upon application of the steady-state approximation to $\bullet\text{OH}$, one gets the following expression for
 261 the initial degradation rate of TBCZ, R_{TBCZ} (see **Figure 2** for the experimental results):

262
$$R_{\text{TBCZ}} = \frac{R_{\text{f},\bullet\text{OH}} k_{\bullet\text{OH}+\text{TBCZ}} C_{\text{TBCZ}}^0}{k_{\bullet\text{OH}+\text{TBCZ}} C_{\text{TBCZ}}^0 + k_{\bullet\text{OH}+\text{H}_2\text{O}_2} C_{\text{H}_2\text{O}_2} + k_{\bullet\text{OH}+2\text{-Prop}} C_{2\text{-Prop}}} + R_{\text{res.}}$$
 (8)

263 where $R_{\text{f},\bullet\text{OH}}$ is the formation rate of $\bullet\text{OH}$ by H_2O_2 photolysis (reaction 3), $k_{\bullet\text{OH}+\text{TBCZ}}$, $k_{\bullet\text{OH}+\text{H}_2\text{O}_2}$, and
 264 $k_{\bullet\text{OH}+2\text{-Prop}}$ the second-order reaction rate constants between $\bullet\text{OH}$ and TBCZ, H_2O_2 , and 2-propanol,
 265 respectively (reactions 4-6), $C_{\text{TBCZ}}^0 = 20 \text{ }\mu\text{M}$ the initial concentration of TBCZ, $C_{\text{H}_2\text{O}_2} = 5 \text{ mM}$ that
 266 of H_2O_2 , and $C_{2\text{-Prop}}$ the initial concentration of 2-propanol.

267



268
 269 **Figure 2.** Trend of the TBCZ initial photodegradation rate (R_{TBCZ}) as a function of the
 270 concentration of 2-propanol ($C_{2\text{-Prop}}$), used as $\bullet\text{OH}$ scavenger. The dashed curve represents data fit
 271 with **Eq. 8**, the solid curves are 95% confidence limits of the fit.

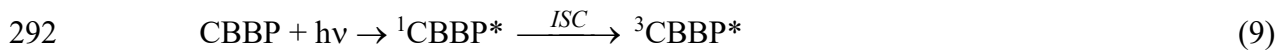
272

273 $R_{\text{res.}}$ is a residual rate value, accounting for possible side reactions of TBCZ (for instance, its direct
 274 photolysis and/or reactions with radicals produced from oxidation of 2-Prop by $\bullet\text{OH}$) (Gornik et al.,
 275 2021). The trend of R_{TBCZ} vs. $C_{2\text{-Prop}}$ is reported in **Figure 2**. The numerical fit of the experimental
 276 data with **Eq. (8)** yielded $k_{\bullet\text{OH}+\text{TBCZ}} = (1.2 \pm 0.3) \times 10^{10} \text{ M}^{-1} \text{ s}^{-1} (\mu \pm \sigma)$, and $R_{\text{t.}\bullet\text{OH}} = (1.6 \pm 0.1) \times 10^{-8} \text{ M}$
 277 s^{-1} .

278

279 *Triplet-sensitised degradation of TBCZ ($^3\text{CBBP}^*$ as $^3\text{CDOM}^*$ proxy)*

280 To assess the potential for TBCZ to be degraded by reaction with $^3\text{CDOM}^*$, here CBBP was used
 281 as proxy of triplet-sensitisation by CDOM, following an already established (Minella et al., 2018)
 282 and validated (Carena et al., 2019) experimental protocol. Irradiation of TBCZ and CBBP under a
 283 UVA lamp triggers the reaction between TBCZ and the CBBP triplet state, $^3\text{CBBP}^*$, while at the
 284 same time minimising the direct photolysis of TBCZ. The problem with CBBP is that it also yields
 285 $^1\text{O}_2$ under irradiation, although with very-well known kinetics (Minella et al., 2018). Therefore, the
 286 degradation of TBCZ by photogenerated $^1\text{O}_2$ is to be taken into account. The overall reaction
 287 system involving CBBP + TBCZ under UVA irradiation can be schematised as follows (ISC: inter-
 288 system crossing; $S_{\Delta} = 0.46$: yield of $^1\text{O}_2$ upon reaction between $^3\text{CBBP}^*$ and O_2 ; $k_{^3\text{CBBP}^*+\text{TBCZ}}$:
 289 second-order reaction rate constant between $^3\text{CBBP}^*$ and TBCZ; $k_{^1\text{O}_2+\text{TBCZ}}$: second-order reaction
 290 rate constant between $^1\text{O}_2$ and TBCZ; k_d : first-order deactivation constant of $^1\text{O}_2$ in aqueous
 291 solution) (Wilkinson and Brummer, 1981; Minella et al., 2018):





299 Upon application of the steady-state approximation to $^3\text{CBBP}^*$ and $^1\text{O}_2$, one gets the following
 300 expression for the degradation rate of the substrate (Minella et al., 2018), TBCZ in the present case:

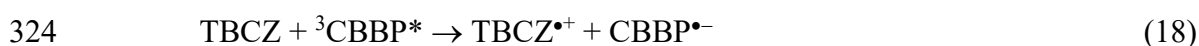
301
$$R_{\text{TBCZ}} = \Phi_{^3\text{CBBP}^*} P_{\text{a,CBBP}} \left(\frac{k_{^3\text{CBBP}^*+\text{TBCZ}} C_{\text{TBCZ}}^{\circ}}{k' + k_{^3\text{CBBP}^*+\text{TBCZ}} C_{\text{TBCZ}}^{\circ}} + \frac{0.68 S_{\Delta} k' k_{^1\text{O}_2+\text{TBCZ}} C_{\text{TBCZ}}^{\circ}}{(k' + k_{^3\text{CBBP}^*+\text{TBCZ}} C_{\text{TBCZ}}^{\circ})(k_d + k_{^1\text{O}_2+\text{TBCZ}} C_{\text{TBCZ}}^{\circ})} \right)$$
 (16)

302 where $\Phi_{^3\text{CBBP}^*} \sim 1$ is the quantum yield of $^3\text{CBBP}^*$ production by irradiated CBBP (Marciniak et
 303 al., 1994), $k' = 6 \times 10^5 \text{ s}^{-1}$ is the first-order rate constant of $^3\text{CBBP}^*$ deactivation in aerated solution,
 304 by internal conversion and reaction with O_2 (Minella et al., 2018), $P_{\text{a,CBBP}} = 1.2 \times 10^{-8} \text{ Einstein L}^{-1}$
 305 s^{-1} is the photon flux absorbed by $67 \mu\text{M}$ CBBP, and 0.68 is the fraction of $^3\text{CBBP}^*$ that gets
 306 inactivated by dissolved oxygen (Minella et al., 2018). Note that the fraction of $^3\text{CBBP}^*$ that is
 307 inactivated by internal conversion is 0.32, while the fraction of $^3\text{CBBP}^*$ that is inactivated by
 308 reaction with TBCZ is negligible, if C_{TBCZ}° is sufficiently low. If C_{TBCZ}° is low enough, one should
 309 get a linear trend of R_{TBCZ} vs. C_{TBCZ}° ($R_{\text{TBCZ}} = m \times C_{\text{TBCZ}}^{\circ}$). Calculation of the line slope m (Minella
 310 et al., 2018) allows for the determination of the second-order rate constant of the reaction between
 311 $^3\text{CBBP}^*$ and TBCZ, $k_{^3\text{CBBP}^*+\text{TBCZ}}$:

312
$$k_{^3\text{CBBP}^*+\text{TBCZ}} = k' \left(\frac{m}{P_{\text{a,CBBP}}} - \frac{0.68 S_{\Delta} k_{^1\text{O}_2+\text{TBCZ}}}{k_d} \right)$$
 (17)

313 The reactivity of TBCZ towards $^1\text{O}_2$ was found to be very low (**Text S2**), thus the term $k_{^1\text{O}_2+\text{TBCZ}}$ in
 314 **Eq. (17)** can be neglected (*i.e.*, $0.68 S_{\Delta} k_{^1\text{O}_2+\text{TBCZ}} (k_d)^{-1} \ll m (P_{\text{a,CBBP}})^{-1}$, from which one gets
 315 $k_{^3\text{CBBP}^*+\text{TBCZ}} \sim k' m (P_{\text{a,CBBP}})^{-1}$). A linear trend of R_{TBCZ} vs. C_{TBCZ}° was observed in the TBCZ
 316 concentration range from 5 to $20 \mu\text{M}$ (see **Figure S5 (SM)**), from which it was possible to obtain
 317 $k_{^3\text{CBBP}^*+\text{TBCZ}} = (2.45 \pm 0.10) \times 10^8 \text{ M}^{-1} \text{ s}^{-1}$.

318 With some substrates, the primary intermediates produced by triplet-sensitised oxidation can be
 319 reduced back to the parent compounds, by phenolic antioxidants (AOs) (Canonica and Laubscher,
 320 2008). In particular, the AO moieties occurring in DOM play a major role in back-reduction. With
 321 phenol (PhOH) as model AO (Wenk and Canonica, 2012), TBCZ as substrate, and CBBP as
 322 CDOM proxy, the back-reduction process (**reaction 20**) would operate as follows, to inhibit the
 323 degradation of TBCZ that initially proceeds through **reactions (18,19)**:



327 The addition of phenol, in the concentration range of 0-50 μM , had a negligible effect on the
 328 degradation of TBCZ sensitised by ${}^3\text{CBBP}^*$, as shown in **Figure S6 (SM)**. Phenol concentration
 329 was not increased above 50 μM , to avoid scavenging of ${}^3\text{CBBP}^*$ by phenol itself (Vione et al.,
 330 2018), which would inhibit the degradation of TBCZ independently of back-reduction. Note that the
 331 AO effect of 50 μM phenol would be approximately equivalent to that of 20 $\text{mg}_\text{C} \text{ L}^{-1}$ DOC in
 332 natural waters (Leresche et al., 2016). Therefore, it can be inferred that TBCZ would not undergo
 333 significant back reduction in environmental conditions.

334

335 ***Predicted photodegradation of TBCZ in sunlit surface waters***

336 Additional experiments suggested that TBCZ would not be degraded by the carbonate radical,
 337 $\text{CO}_3^{\bullet-}$, to a significant extent (see **Text S3 (SM)**). Therefore, TBCZ in natural surface freshwaters
 338 would mainly be degraded by $^{\bullet}\text{OH}$, ${}^3\text{CDOM}^*$, and perhaps the direct photolysis. Our innovative
 339 approach consists in predicting the contribution of the different photoreaction pathways to the
 340 photodegradation of TBCZ, by means of the photochemical model contained in APEX, at the same
 341 time assessing the overall lifetime of this compound. By so doing, we surmise that the
 342 environmental photo-fate of TBCZ is affected by environmental factors such as seasonal light

intensity, water depth, and DOM concentration in water, and are able to quantify the role of each factor.

Figure 3 reports an example of the modelled photodegradation kinetics and pathways of TBCZ, under summertime irradiation conditions. It is shown that reaction with $\bullet\text{OH}$ would be the main TBCZ photodegradation pathway, followed by $^3\text{CDOM}^*$ especially at high DOC. In contrast, direct photolysis and reactions with $^1\text{O}_2$ or $\text{CO}_3^{\bullet-}$ would be minor to negligible.

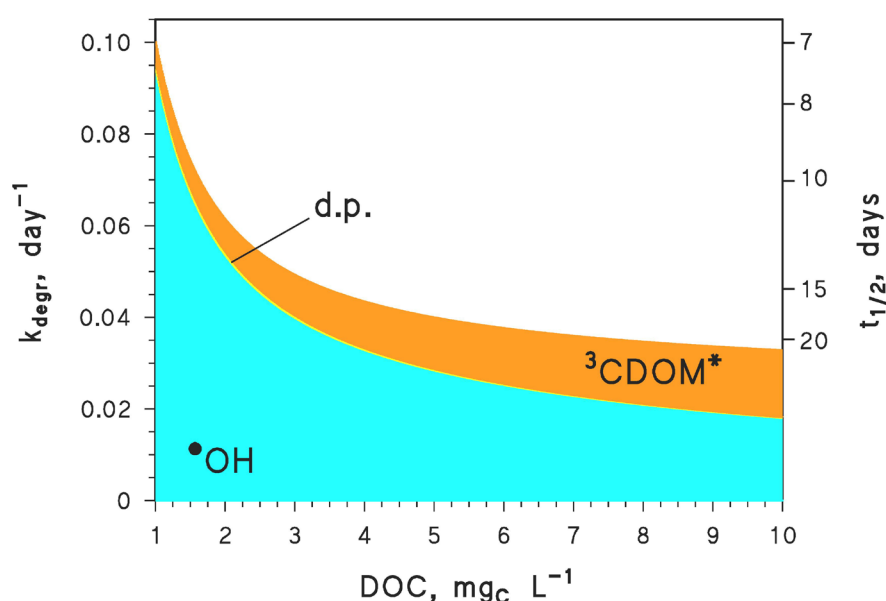
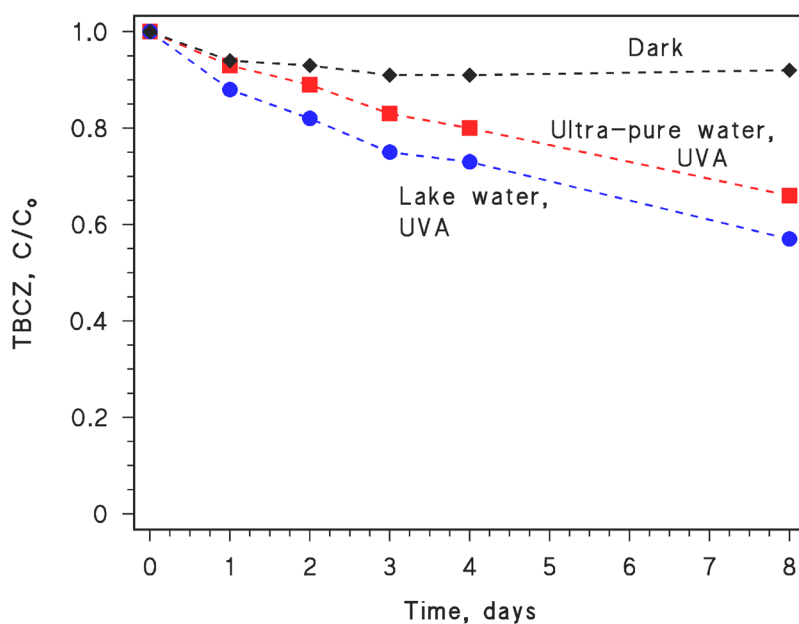


Figure 3. Modelled first-order photodegradation rate constants of TBCZ (k_{degr} , left Y-axis), together with the corresponding half-life times (right Y-axis) ($t_{1/2} = \ln 2 \ k_{\text{degr}}^{-1}$), as a function of the dissolved organic carbon (DOC). Assumed water conditions: depth $d = 1$ m, $[\text{NO}_3^-] = 10^{-4}$ M, $[\text{NO}_2^-] = 10^{-6}$ M, $[\text{HCO}_3^-] = 10^{-3}$ M, $[\text{CO}_3^{2-}] = 10^{-5}$ M. Days correspond to fair-weather 15 July at 45°N latitude. Calculations were carried out with the APEX software; the coloured areas of the graph highlight the importance of the different photodegradation pathways (d.p. = direct photolysis).

360 The resulting TBCZ lifetime would be in the range of days to weeks, varying depending on the
 361 environmental conditions. In particular, given the major role of $\bullet\text{OH}$ in TBCZ photodegradation, the
 362 process would be favoured in shallow, nitrate- and nitrite-rich environments (Zepp et al., 1987) with
 363 low DOC. For instance, with the same water chemistry and sunlight irradiance conditions used in
 364 **Figure 3**, but with water depth $d = 5$ m instead of 1 m, the lifetime ($t_{1/2}$) of TBCZ would increase to
 365 20-70 days (see **Figure S8 (SM)**).

366 The predicted prevalence of indirect over direct TBCZ photodegradation is consistent with the
 367 results of irradiation experiments, in which TBCZ was UVA-irradiated in both ultra-pure water and
 368 lake water. Indeed, TBCZ photodegradation was faster in lake water, as shown in **Figure 4**, which
 369 suggests an important role played by lake-water photosensitisers over the direct photolysis process,
 370 which is the only operational reaction pathway occurring in ultra-pure water.

371



372

373 **Figure 4.** TBCZ time trend upon UVA irradiation, in (■) ultra-pure water and (●) lake water (Lake
 374 Soprano, Western Italian Alps, 2100 m a.s.l.; water chemistry: $25 \mu\text{M NO}_3^-$, $1 \mu\text{M NO}_2^-$, 0.84 mgC
 375 L^{-1} DOC, 1.1 mgC L^{-1} inorganic carbon, pH 6.8). For comparison, the TBCZ time trend in lake
 376 water in the dark (◆) is also reported. UVA irradiance was 25 W m^{-2} .

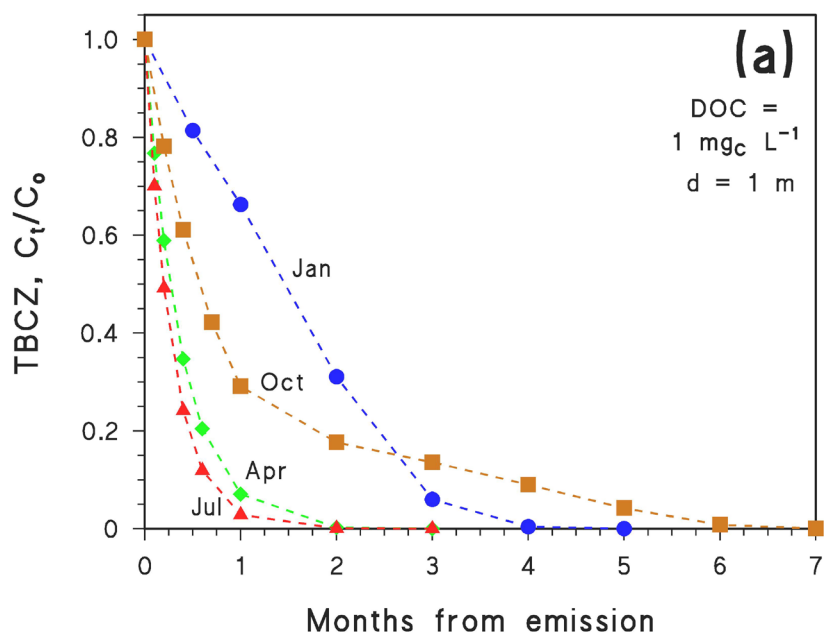
377

378 The results reported in **Figure 3** suggest that TBCZ photodegradation might take more than one
379 month to complete in some environments. In these circumstances, the time trend can be described
380 by **Eq. (1)**, as series of first-order degradation intervals where the rate constant k_m changes from one
381 month to the following (Vione, 2021). Using *APEX_Season* to derive k_m , and applying **Eq. (1)**, one
382 gets the time trends shown in **Figure 5a/b**. In particular, **Figure 5a** was obtained by assuming the
383 most favourable conditions to photodegradation, among those modelled in **Figure 3** (depth $d = 1$ m,
384 $\text{DOC} = 1 \text{ mgC L}^{-1}$). Conversely, in the case of **Figure 5b**, the least favourable conditions among
385 those of **Figure 3** were assumed ($d = 1$ m, $\text{DOC} = 10 \text{ mgC L}^{-1}$).

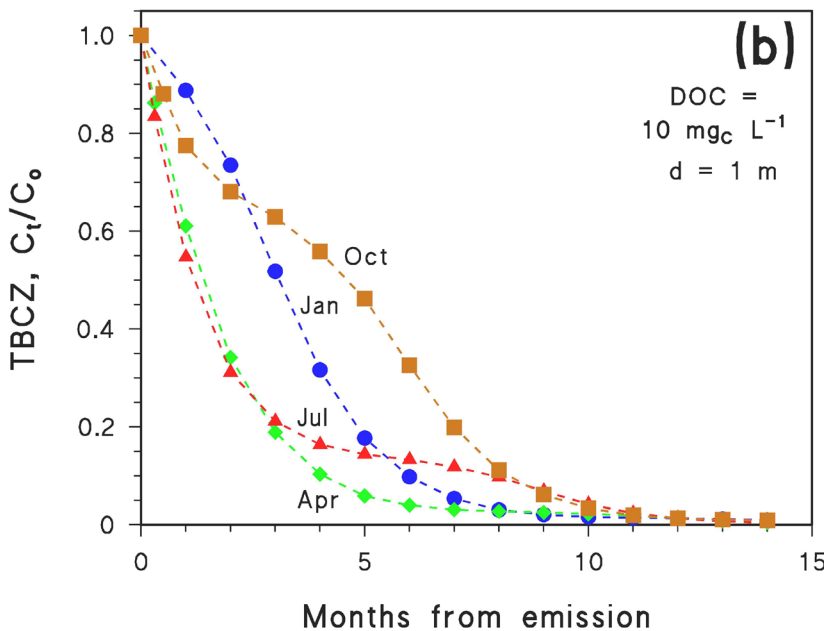
386 Interestingly, if environmental conditions allow TBCZ photodegradation to be relatively fast
387 (**Figure 5a**), extensive removal ($\geq 95\%$) is obtained more quickly if initial emission takes place in
388 summer or spring compared to autumn or winter, as expected (the irradiance of sunlight is in fact
389 higher in spring/summer compared to autumn/winter). In contrast, for slower photodegradation
390 kinetics (**Figure 5b**), one has that $\geq 95\%$ removal is obtained faster for emission in winter or spring,
391 compared to summer or autumn. Actually, in this case photodegradation spans over several months,
392 and the conditions of the initial month/season of emission play more limited role. Indeed, the
393 irradiance conditions of the following season(s) are comparatively more important. **Figure 5b**
394 additionally suggests that, with $d = 1$ m and $\text{DOC} = 10 \text{ mgC L}^{-1}$, it would take from 6-7 months to
395 about 1 year for photodegradation to eliminate TBCZ from the water environment.

396

397



398



399

400

401 **Figure 5.** Modelled time trends of TBCZ photodegradation (Eq. 1), as a function of the month of
402 initial emission ($m = 0$, highlighted near each curve). (a) Depth $d = 1$ m, DOC = 1 mgC
403 L⁻¹; (b) $d = 1$ m, DOC = 10 mgC L⁻¹. Other water conditions: $[\text{NO}_3^-] = 10^{-4}$ M, $[\text{NO}_2^-] =$
404 10^{-6} M, $[\text{HCO}_3^-] = 10^{-3}$ M, and $[\text{CO}_3^{2-}] = 10^{-5}$ M. Consistent fine weather was
405 hypothesised here.

406

407 **Identification of TBCZ phototransformation products**

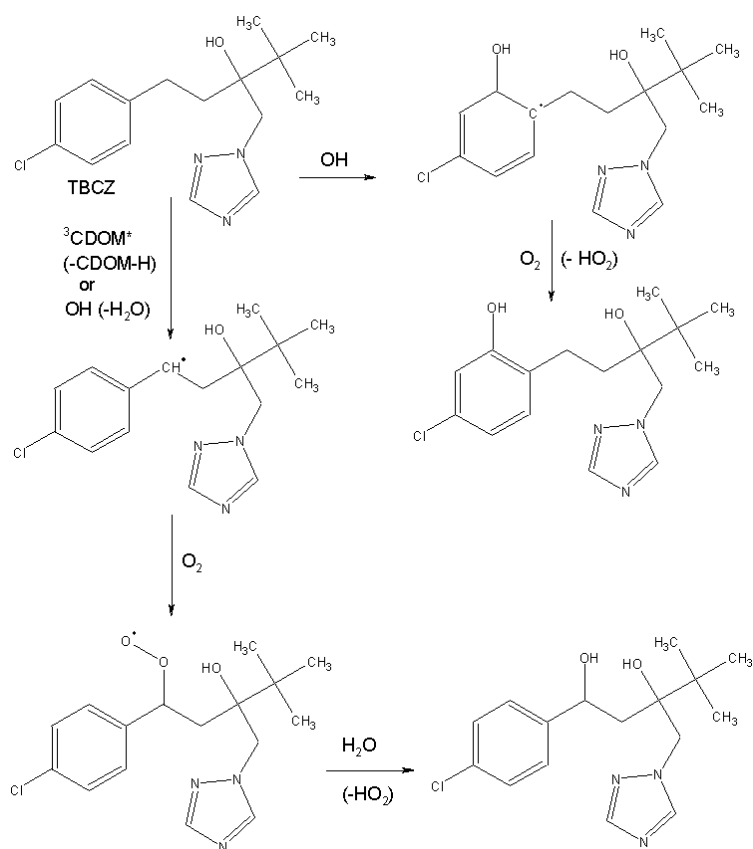
408 In the direct photolysis of TBCZ, only the ion at m/z 308 ($[M + H]^+$) was detected, i.e., parent
 409 TBCZ (see **Table 1** for its fragmentation). The fragment ion at m/z 290 resulted from the loss of a
 410 water molecule from the parent ion, while the fragment m/z 221 was obtained through the loss of
 411 1,2,4-triazacyclo-2,4-pentadiene from m/z 290. Moreover, the loss of butyl gives the ion with m/z
 412 165 (Calza et al., 2002) (see **Figure S9 (SM)**). In the MS³ experiment, the ion at m/z 130 could be
 413 produced by loss of chlorine.

414 The main ions found in the degradation of TBCZ by \bullet OH are reported in **Table 1**, while the
 415 hypothesised structures of the related products are shown in **Table 2**. Identification was possible
 416 thanks to comparison with literature findings, referred to the heterogeneous photocatalytic (TiO₂ +
 417 hv) degradation of TBCZ (Calza et al., 2002). For the details about photoproducts identification by
 418 LC-MSⁿ, the reader is referred to the work by Calza et al. (2002), and to the SM of the present
 419 work.

420 The only degradation products detected with ³CBBP* were two hydroxyderivatives, with ions
 421 having m/z 324 (see **Table 1**). Both ions showed loss of two water molecules (m/z 306 and 288),
 422 and the subsequent loss of triazole (m/z 237) in MS² experiments. The formation of TBCZ
 423 hydroxyderivatives upon reaction with ³CBBP* needs some explanation. The TBCZ alkyl chain
 424 could be oxidised by ³CBBP* via hydrogen transfer, giving a radical species that could add oxygen.
 425 Further reaction with water could then produce the hydroxyderivative(s), and the overall process
 426 (**reactions 21-24**) simulates \bullet OH attack (De Laurentiis et al., 2012 & 2014):



431 Tentative pathways leading to TBCZ hydroxylation, upon reaction with either $\bullet\text{OH}$ or $^3\text{CDOM}^*$, are
432 reported in **Scheme 1**. Note the partial overlap between the $\bullet\text{OH}$ and $^3\text{CDOM}^*$ reactions.



433
434 **Scheme 1.** Tentative reaction pathways leading to the detected TBCZ hydroxyderivatives,
435 involving either $\bullet\text{OH}$ or $^3\text{CDOM}^*$. The attack position of $\bullet\text{OH}$ on the aromatic ring of TBCZ is
436 highly uncertain (the shown position, in *meta* to chlorine, is just an arbitrary assumption).

437
438 Based on the structures of TBCZ and its identified products, ECOSAR calculations (Mayo-Bean et
439 al., 2012) provided insights into their potential acute (values of lethal concentration LC50 and
440 effective concentration EC50) and chronic (chronic value ChV) toxicity, towards freshwater
441 organisms. Calculation results are reported in **Table 2**, and they represent an order-of-magnitude
442 estimate of toxicity values (Mayo-Bean et al., 2012). On this basis, the obtained results suggest that
443 TBCZ phototransformation products have similar or lower toxicity compared to their parent
444 compound. A decrease in toxicity is expected, especially after fragmentation of the aromatic ring.
445 Therefore, TBCZ photodegradation is likely to lead to detoxification.

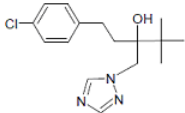
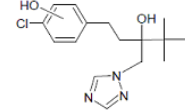
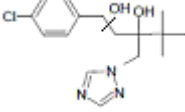
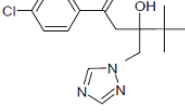
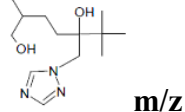
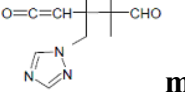
446 **Table 1.** Main fragmentations in MSⁿ of TBCZ and its degradation products, because of direct
 447 photolysis (48 hours of irradiation), •OH reaction (30 minutes of irradiation), and reaction with
 448 ³CBBP* (48 hours of irradiation).
 449

Photochemical conditions	MS ² (m/z)	MS ³ (m/z)	Retention time (min)	Ions m/z, relative abundance in brackets (referred to the most intense ion)
d.p.	308*	-	20.92	290 (24), 221 (23), 181 (24), 165 (100), 151 (22), 139 (15), 125 (55)
	308**	165	20.64	130 (100)
•OH	324	306	19.66	306 (100), 288(36), 237 (26), 181 (75), 167 (38), 141 (45), 109 (5)
	324	306	18.86	306 (70), 237 (15), 196 (12), 181 (100), 167 (93), 155 (9), 141 (5)
	324	306	16.00	322 (10), 305 (8), 288 (23), 280 (43), 263 (100), 237 (9), 181 (18)
	322	304	20.64	304 (8), 286 (5), 235 (100), 179 (12), 139 (8)
	278	260	16.57	260 (9), 242 (12), 191 (91), 178 (100), 173 (62), 145 (46), 109 (36), 107 (31), 95 (10)
	272	236	12.53	180 (18), 167 (100), 162 (19), 137 (7), 111 (45), 83 (10), 70 (31)
	224	206	14.33	206 (16), 178 (6), 137 (100), 109 (9), 107 (14), 70 (46)
³ CDOM* (³ CBBP*)	324	-	20.36	306 (6), 288 (100), 237(10), 207 (33), 177 (19), 168 (23), 151 (13), 139 (29)
	324	-	19.90	306 (44), 288 (100), 237 (1), 168 (23)

450 * Summary of MS² experiment for TBCZ. ** Summary of MS³ experiment for TBCZ.

451

Table 2. Acute (LC50/EC50) and chronic (ChV) toxicity values (mg L⁻¹ units) of TBCZ and its detected phototransformation products, calculated by means of the ECOSAR software, on the basis of molecular structures. The m/z values refer to the [M+H]⁺ molecular ions, which are discussed in the text (the reported structures show the neutral molecules M). The reported values are here the lowest, among the multiple classes that ECOSAR can identify for a given compound.

	Fish		Crustaceans		Algae	
	LC50	ChV	LC50	ChV	EC50	ChV
 TBCZ	2.4	0.02	3.5	0.19	0.9	0.5
 m/z 324b	4.7	0.04	3.9	0.4	0.4	0.7
 m/z 324a/c	19.6	0.09	17.6	1.3	3.3	1.3
 m/z 322	6.1	0.1	4.6	0.6	1.4	1.6
 m/z 272	1,090	1.9	377	45.5	40.9	7.7
 m/z 224	56.9	37.4	233	6.8	12.3	42.2

Conclusions

The fungicide TBCZ does not undergo direct photolysis to a significant extent in environmental conditions. From measured photoreactivity parameters (which are summarised in **Table S2(SM)**), it can be inferred that the main TBCZ phototransformation processes in sunlit surface waters are the reactions with $\bullet\text{OH}$ (especially) and $^3\text{CDOM}^*$. In the latter case, no back-reduction of partially oxidised TBCZ is expected to be operated by the phenolic antioxidant moieties occurring in DOM. Therefore, no inhibition of $^3\text{CDOM}^*$ degradation by DOM phenols should take place in high-DOC waters. The photochemical lifetime of TBCZ in the natural environment would strongly depend on the environmental conditions. The value of $t_{1/2}$ could be as low as one week under favourable circumstances (shallow waters with low DOC during summertime, when degradation by $\bullet\text{OH}$ is highly enhanced). Conversely, the inhibition of the $\bullet\text{OH}$ process at high DOC ($\bullet\text{OH}$ is in fact efficiently scavenged by DOM) is only partially offset by the enhancement of degradation by $^3\text{CDOM}^*$. In these conditions, TBCZ degradation could span over several months, departing from first-order kinetics, because of seasonally changing irradiance of sunlight. TBCZ elimination could thus require 6-7 months, upon initial emission in winter or spring, and up to one year if initial emission takes place in summer or autumn.

The phototransformation of TBCZ has potential to lower its environmental impact, when judging from the expected toxicity of the detected products. In particular, TBCZ photodegradation mainly proceeds by hydroxylation, followed by fragmentation of the aromatic ring.

References

- Avetta, P., Fabbri, D., Minella, M., Brigante, M., Maurino, V., Minero, C., Pazzi, M., Vione, D., 2016. Assessing the phototransformation of diclofenac, clofibric acid and naproxen in surface waters: Model predictions and comparison with field data. *Water Res.* 105, 383-394.
- Baena-Nogueras, R. M., Gonzalez-Mazo, E., Lara-Martin, P. A., 2017. degradation kinetics of pharmaceuticals and personal care products in surface waters: photolysis vs. biodegradation. *Sci. Total Environ.* 590-591, 643-654.
- Bodrato, M.; Vione, D., 2014. APEX (Aqueous Photochemistry of Environmentally occurring Xenobiotics): a free software tool to predict the kinetics of photochemical processes in surface waters. *Environ. Sci.-Process Impacts* 16, 732-740.
- Boethling, R. S., Lynch, D. G., Jaworska, J. S., Tunkel, J. L., Thom, G. C., Webb, S., 2004. Using BIOWIN, Bayes, and batteries to predict ready biodegradability. *Environ. Toxicol. Chem.* 23, 911-920.
- Braslavsky, S. E., 2007. Glossary of terms used in photochemistry. third edition. *Pure Appl. Chem.* 79, 293-465.
- Buxton, G. V, Greenstock, C.L., Helman, P.W., Ross, A.B., 1988. Critical Review of rate constants for reactions of hydrated electrons, hydrogen atoms and hydroxyl radicals ($\cdot\text{OH}/\cdot\text{O}$ -) in Aqueous Solution. *J. Phys. Chem. Ref. Data* 17, 513-886.
- Calza, P., Baudino, S., Aigotti, R., Baiocchi, C., Branca, P., Pelizzetti, E., 2002. High-performance liquid chromatographic/tandem mass spectrometric identification of the phototransformation products of tebuconazole on titanium dioxide. *J. Mass Spectrom.* 37, 566-576.
- Canonica, S., Kohn, T., Mac, M., Real, F. J., Wirz, J., Von Gunten, U., 2005. Photosensitizer method to determine rate constants for the reaction of carbonate radical with organic compounds. *Environ. Sci. Technol.* 39, 9182-9188.
- Canonica, S., Laubscher, H.U., 2008. Inhibitory effect of dissolved organic matter on triplet-induced oxidation of aquatic contaminants. *Photochem. Photobiol. Sci.* 7, 547-551.
- Carena, L., Puscasu, C.G., Comis, S., Sarakha, M., Vione, D., 2019. Environmental photodegradation of emerging contaminants: A re-examination of the importance of triplet-sensitised processes, based on the use of 4-carboxybenzophenone as proxy for the chromophoric dissolved organic matter. *Chemosphere* 237, 124476.
- Carena, L., Vione, D., Minella, M., Canonica, S., Schönenberger, U., 2022. Inhibition by phenolic antioxidants of the degradation of aromatic amines and sulfadiazine by the carbonate radical ($\text{CO}_3^{\cdot-}$). *Water Res.* 209, 117867.

Coody, P. N., 1987. Photodecomposition of Folicur in soil and water. Mobay Chemical Corporation, Stilwell, KS, USA. Bayer CropScience AG, Edition Number: M-005404-01-1.

Cory, R. M., Cotner, J. B., McNeill, K., 2009. Quantifying interactions between singlet oxygen and aquatic fulvic acids. *Environ. Sci. Technol.* 43, 718-723.

De Laurentiis, E., Chiron, S., Kouras-Hadef, S., Richard, C., Minella, M., Maurino, V., Minero, C., Vione, D., 2012. Photochemical fate of carbamazepine in surface freshwaters: laboratory measures and modelling. *Environ. Sci. Technol.* 46, 8164-8173.

De Laurentiis, E., Prasse, C., Ternes, T. A., Minella, M., Maurino, V., Minero, C., Sarakha, M., Brigante, M., Vione, D., 2014. Assessing the photochemical transformation pathways of acetaminophen relevant to surface waters: transformation kinetics, intermediates, and modelling. *Water Res.* 53, 235-248.

DeRosa, M. C., Crutchley, R. J., 2002. Photosensitized singlet oxygen and its applications. *Coord. Chem. Rev.* 233-234, 351-371.

Dong, M. M., Rosario-Ortiz, F. L., 2012. Photochemical formation of hydroxyl radical from effluent organic matter. *Environ Sci Technol.* 46, 3788-3794.

EFSA (European Food Safety Agency), 2008. Conclusion regarding the peer review of the pesticide risk assessment of the active substance tebuconazole. *EFSA J.* 12, 3485–3583.

Fera, M. T., La Camera, E., Desarro, A., 2009. New triazoles and echinocandins: Mode of action, in vitro activity and mechanisms of resistance. *Expert Rev. Anti-infect. Ther.* 7, 981-998.

Galbavy, E.S., Ram, K., Anastasio, C., 2010. 2-Nitrobenzaldehyde as a chemical actinometer for solution and ice photochemistry. *J. Photochem. Photobiol. A Chem.* 209, 186-192.

Gligorovski, S., Strekowski, R., Barbati, S., Vione, D., 2015. Environmental implications of hydroxyl radicals ($\cdot\text{OH}$). *Chem. Rev.* 115, 13051-13092.

Gornik, T., Carena, L., Kosjek, T., Vione, D., 2021. Phototransformation study of the antidepressant paroxetine in surface waters. *Sci. Total Environ.* 774, 145380.

Hao, Z., Ma, J., Miao, C., Song, Y., Lian, L., Yan, S., Song, W., 2020. Carbonate radical oxidation of cylindrospermopsin (cyanotoxin): Kinetic studies and mechanistic consideration. *Environ. Sci. Technol.* 54, 10118–10127.

Kahle, M., Buerge, I. J., Hauser, A., Müller, M. D., Poiger, T., 2008. Azole fungicides: occurrence and fate in wastewater and surface waters. *Environ. Sci. Technol.* 42, 7193-7200.

Leresche, F., von Gunten, U., Canonica, S., 2016. Probing the photosensitizing and inhibitory effects of dissolved organic matter by using N,N-dimethyl-4-cyanoaniline (DMABN). *Environ. Sci. Technol.* 50, 10997-11007.

535 Lyu, T., Zhang, L., Xu, X., Arias, C.A., Brix, H., Carvalho, P.N., 2018. Removal of the pesticide
536 tebuconazole in constructed wetlands: Design comparison, influencing factors and modelling.
537 Environ. Pollut. 233, 71-80.

538 Marciniak, B., Bobrowski, K., Hug, G. L., Rozwadowski, J., 1994. Photoinduced electron transfer
539 between sulfur-containing carboxylic acids and 4-carboxybenzophenone triplet state in
540 aqueous solutions. J. Phys. Chem. 98, 4854-4860.

541 Mayo-Bean, K., Moran, K., Meylan, B., Ranslow, P., 2012. Methodology document for the
542 ECOlogical Structure-activity Relationship model (ECOSAR) class program. US-EPA,
543 Washington DC, 46 pp.

544 McNeill, K., Canonica, S., 2016. Triplet state dissolved organic matter in aquatic photochemistry:
545 reaction mechanisms, substrate scope, and photophysical properties. Environ. Sci.-Processes
546 Impacts 18, 1381-1399.

547 Miyauchi, T., Mori, M., Ito, K., 2005. Application of solid-phase extraction to quantitatively
548 determine cyproconazole and tebuconazole in treated wood using liquid chromatography with
549 UV detection. J. Chromatogr. A 1063, 137-141.

550 Minella, M., Rapa, L., Carena, L., Pazzi, M., Maurino, V., Minero, C., Brigante, M., Vione, D.,
551 2018. An experimental methodology to measure the reaction rate constants of processes
552 sensitised by the triplet state of 4-carboxybenzophenone as a proxy of the triplet states of
553 chromophoric dissolved organic matter, under steady-state irradiation conditions. Environ.
554 Sci.: Processes Impacts 20, 1007-1019.

555 Mostafa, S., Rosario-Ortiz, F. L., 2013. Singlet oxygen formation from wastewater organic matter.
556 Environ Sci Technol. 47, 8179-8186.

557 Muñoz-Leoz, B., Ruiz-Romera, E., Antigüedad, I., Garbisu, C., 2011. Tebuconazole application
558 decreases soil microbial biomass and activity. Soil Biol. Biochem. 43, 2176-2183.

559 Paul, P. A., Lipps, P. E., Hershman, D. E., McMullen, M. P., Draper, M. A., Madden, L. V., 2008.
560 Efficacy of triazole-based fungicides for fusarium head blight and deoxynivalenol control in
561 wheat: a multivariate meta-analysis. Phytopathology 98, 999-1011.

562 Remucal, C. K., 2014. The role of indirect photochemical degradation in the environmental fate of
563 pesticides: a review. Environ. Sci.: Processes Impacts 16, 628-653.

564 Rosario-Ortiz, F. L., Canonica, S., 2016. Probe compounds to assess the photochemical activity of
565 dissolved organic matter. Environ. Sci. Technol. 50, 12532-12547.

566 Vione, D., Khanra, S., Cucu Man, S., Maddigapu, P. R., Das, R., Arsene, C., Olariu, R. I., Maurino,
567 V., Minero, C., 2009. Inhibition vs. enhancement of the nitrate-induced phototransformation

of organic substrates by the $\bullet\text{OH}$ scavengers bicarbonate and carbonate. *Water Res.* 43, 4718-4728.

Vione, D., Sur, B., Dutta, B. K., Maurino, V., Minero, C., 2011. On the effect of 2-propanol on phenol photonitration upon nitrate photolysis. *J. Photochem. Photobiol. A: Chem.* 224, 68-70.

Vione, D., Minella, M., Maurino, V., Minero, C., 2014. Indirect photochemistry in sunlit surface waters: photoinduced production of reactive transient species. *Chem.-Eur. J.* 20, 10590-10606.

Vione, D., Fabbri, D., Minella, M., Canonica, S., 2018. Effects of the antioxidant moieties of dissolved organic matter on triplet-sensitized phototransformation processes: Implications for the photochemical modeling of sulfadiazine. *Water Res.* 128, 38-48.

Vione, D., Scozzaro, A., 2019. Photochemistry of surface fresh waters in the framework of climate change. *Environ. Sci. Technol.* 53, 7945-7963.

Vione, D., 2021. Insights into the time evolution of slowly photodegrading contaminants. *Molecules* 26, 5223.

Wenk, J., Von Gunten, U., Canonica, S., 2011. Effect of Dissolved Organic Matter on the Transformation of Contaminants Induced by Excited Triplet States and the Hydroxyl Radical. *Environ. Sci. Technol.* 45, 1334-1340.

Wenk, J., Canonica, S., 2012. Phenolic antioxidants inhibit the triplet-induced transformation of anilines and sulfonamide antibiotics in aqueous solution. *Environ. Sci. Technol.* 46, 5455-5462.

Wenk, J., Eustis, S. N., McNeill, K., Canonica, S., 2013. Quenching of excited triplet states by dissolved natural organic matter. *Environ. Sci. Technol.* 47, 12802-12810.

Wiche, A., Bogdoll, B., 2007. Tebuconazole (AE F069623) Abiotic degradation, hydrolysis as a function of pH. Bayer CropScience AG, Frankfurt am Main, Germany, Edition Number: M-295245-01-1.

Wilkinson, F., Brummer, J., 1981. Rate constants for the decay and reactions of the lowest electronically excited singlet-state of molecular oxygen in solution. *J. Phys. Chem. Ref. Data* 10, 809-1000.

Willett, K. L., Hites, R. A., 2000. Chemical actinometry: Using o-nitrobenzaldehyde to measure lamp intensity in photochemical experiments. *J. Chem. Educ.* 77, 900.

Yan, S., Song, W., 2014. Photo-transformation of pharmaceutically active compounds in the aqueous environment: a review. *Environ. Sci.: Processes Impacts* 16, 697-720.

Yan, S., Liu, Y., Lian, L., Li, R., Ma, J., Zhou, H., Song, W., 2019. Photochemical formation of carbonate radical and its reaction with dissolved organic matters. *Water Res.* 161, 288-296.

601 Yu, L., Chen, M., Liu, Y., Gui, W., Zhu, G., 2013. Thyroid endocrine disruption in zebrafish larvae
602 following exposure to hexaconazole and tebuconazole. *Aquat. Toxicol.* 138, 35-42.

603 Želonková, K., Havadej, S., Verebová, V., Holečková, B., Uličný, J., Staničová, J., 2019. Fungicide
604 tebuconazole influences the structure of human serum albumin molecule. *Molecules* 24, 3190.

605 Zellner, R., Exner, M., Herrmann, H., 1990. Absolute OH quantum yields in the laser photolysis of
606 nitrate, nitrite and dissolved H₂O₂ at 308 and 351 nm in the temperature range 278-353 K. *J.*
607 *Atmos. Chem.* 10, 411-425.

608 Zepp, R. G., Hoigné, J., Bader, H., 1987. Nitrate-induced photooxidation of trace organic chemicals
609 in water. *Environ. Sci. Technol.* 21, 443-450.